

Research on a Novel Radial Magnetic Bearing

Zong Ming, Wang Fengxiang, Wang Jiqiang, Sun Yidan
Shenyang University of Technology, Shenyang 110023, China
Tel/Fax: 86-24-25691433, 86-24-25691432
E-mail: ming_zong@613.com zong_ming@hotmail.com

Author Information

Zong Ming was born in Shenyang, China, 1957. He received the B.S. degree from Shenyang University of Technology, China, in 1982, and the M.S. degree from Northeast University, China, in 1995, both in Electrical engineering. Since 1982, Zong Ming has been serving as a teacher to the school of Electrical Engineering at Shenyang University of Technology. His main research interests and experience include analysis and design of electrical apparatus, control system, modeling, simulation and power converter. He was a Visiting Professor at the Fachhochschule Esslingen-Hochschule für Technik, University of Applied Sciences, Esslingen, Germany from 2002 to 2003.

Key words: radial magnetic bearing, PID controller, simulation, magnetic levitation

Abstract: In this paper, the structure of a novel radial magnetic bearing without individual displacement sensor is proposed. The operating principle of this kind of radial magnetic bearing is also introduced. The stability of the radial magnetic bearing is analyzed by the control system theory. The analysis shows that the proposed system is instable in dynamic state process. The simulation study on an example shows that the radial magnetic bearing proposed can levitate stably by means of a PD controller. But it is a system with steady-state error.

1 Introduction

Magnetic bearing are designed to support rotating and linear moving machinery elements without coming into contact with the rotor. This is accomplished by applying the principle that an electromagnet will attract a ferromagnetic material. Using this principle the rotor can be suspended in a magnetic field which is generated by the bearing.

A typical radial active magnetic bearing consists of stator, sensor mounted over the rotor and control system. The rotor position can be controlled by the control system according to measuring results of the displacement sensor. In the novel radial magnetic bearing proposed in this paper, the individual displacement sensor is not needed. Only using the capacitors in series with stator windings of the magnetic bearing and high frequency AC power supply, the magnetic bearing design can be simplified and the rotor levitation can be achieved in the steady-state. Because of the dynamic state instability, PD controller is required. The change of the rotor position can be gotten by measuring the current in stators winding.

2 Structure of the radial magnetic bearing

The structure of the radial magnetic bearing proposed in this paper is shown in Fig.1.

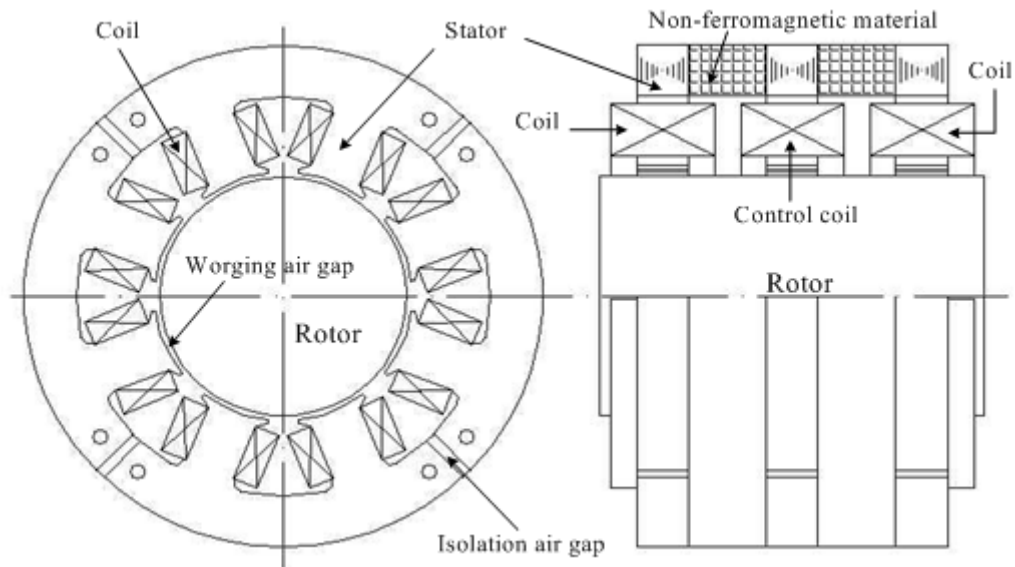


Fig.1 Structure of the radial active magnetic bearing proposed

The characteristics of the radial magnetic bearing in structure are:

- 12 pairs of the magnetic poles are insulated by the isolation air gaps to reduce magnetic coupling between different poles.
- In order to eliminate variation of the electromagnetic force caused by AC excitation, two twin magnetic circuits insulated by non-ferromagnetic material are adopted.
- A set of the control winding is used to improve the dynamic response of the magnetic bearing.

3 Operating Principle of the radial magnetic bearing

Fig.2 is the schematic diagram of the radial magnetic bearing for one degree of freedom (DOF).

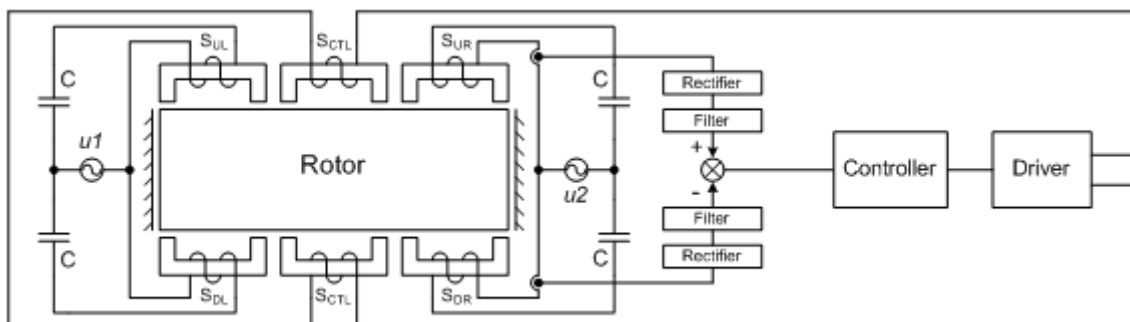


Fig.2. Schematic diagram of the radial magnetic bearing proposed

S_{UL} , S_{UR} , S_{DL} and S_{DR} represent the top left electromagnet, top right electromagnet, bottom left electromagnet and bottom right electromagnet respectively. The $u1$ is an AC power supply for left electromagnets and the $u2$ is for right electromagnets. C is the capacitor in series with the electromagnet winding of the magnetic bearing. It can be selected from equation 1.

$$C = \frac{1}{\omega^2 \times L_{\min} \times K_c} \quad (0.7 < K_c < 1) \quad (1)$$

Where ω = the angular frequency of the AC power supply, L_{\min} = minimum inductance within the bound of rotor moving.

In the case of reluctance of iron core and fringing flux are ignored, the inductance of the electromagnet winding can be written as

$$L = \frac{\mu_0 \times S}{2\delta} \times N^2 \quad (2)$$

Where S = the cross-sectional area of the stator core, N = the winding turns, δ = working air gap length.

The peak amplitude of the steady-state current in any electromagnet winding is given as

$$I_m = \frac{U_m}{\sqrt{R^2 + \left(\omega L - \frac{1}{\omega C}\right)^2}} \quad (3)$$

Where U_m = the voltage peak amplitude of the AC power supply, R = the resistance of the winding.

From equation 3, the relationship between inductance L (i.e. air gap length, see equation 2) and current in any electromagnet winding is shown in Fig.3.

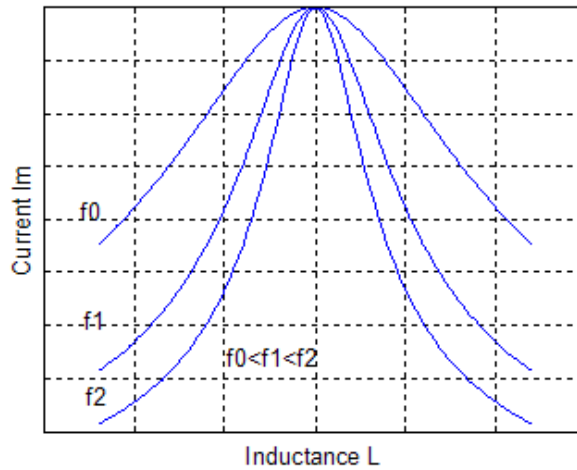


Fig.3 Relationship curve between inductance and current in an electromagnet

Where $f_0 \sim f_2$ = frequency of the AC power supply in Hz.

The peak amplitude current through an electromagnet winding occurs when $\omega L = 1/\omega C$. From Fig.3, as long as the inductance variation is limited in the bound of right hand side of Fig.3, the steady-state current amplitude through an electromagnet winding will be reduced with inductance increasing rapidly.

When the working air gap length is smaller, the magnetic attracting force to rotor produced by the top left electromagnet is

$$F_{UL} = \frac{\varphi^2}{\mu_0 S} = \frac{\Phi_m^2}{\mu_0 S} \sin^2 \omega t = \frac{\Phi_m^2}{2\mu_0 S} - \frac{\Phi_m^2}{2\mu_0 S} \cos 2\omega t = F_{ULm} - F_{ULm} \cos 2\omega t \quad (4)$$

Where ω = the alternating magnetic flux. ϕ_m = the peak amplitude of the alternating magnetic flux.

Owing to the magnetic attracting force, F_{UL} , is fluctuating, the rotor pulsate is occurred. In order to eliminate variation of the electromagnetic force caused by alternating magnetic flux, another alternating magnetic flux with 90 degree phase difference is applied to the top right electromagnet. So the magnetic attracting force to rotor produced by this electromagnet is

$$F_{UR} = \frac{\Phi^2}{\mu_0 S} = \frac{\Phi_m^2}{\mu_0 S} \cos^2 \omega t = \frac{\Phi_m^2}{2\mu_0 S} + \frac{\Phi_m^2}{2\mu_0 S} \cos 2\omega t = F_{URm} + F_{URm} \cos 2\omega t \quad (5)$$

The resultant force acting on the rotor produced by top electromagnet can be written as

$$F_U = F_{UR} + F_{UL} = \frac{\Phi_m^2}{\mu_0 S} = \frac{\mu_0 S}{4\delta_u^2} N^2 I_{um}^2 \quad (6)$$

Where δ_u = the upper working air gap length, I_{um} = the peak amplitude of the steady-state current in upper electromagnet windings.

Equation 6 shows the resultant force produced by top electromagnets is invariable.

According to the structure symmetry, the resultant force acting on the rotor produced by bottom electromagnets can be written as

$$F_D = F_{DR} + F_{DL} = \frac{\Phi_m^2}{\mu_0 S} = \frac{\mu_0 S}{4\delta_d^2} N^2 I_{dm}^2 \quad (7)$$

Where δ_d = the subjacent working air gap length, I_{dm} = the peak amplitude of the steady-state current in subjacent electromagnet windings.

Under no excitation in the control winding, S_{CTR} , the resultant force acting on the rotor can be written

$$\begin{aligned} F &= F_D - F_U = \frac{1}{4} \mu_0 S N^2 \left(\frac{I_{um}^2}{\delta_u^2} - \frac{I_{dm}^2}{\delta_d^2} \right) \\ &= K_0 \left[\frac{1}{K_1 (a+x)^2 + K_2 (b-x)^2} - \frac{1}{K_1 (a-x)^2 + K_2 (b+x)^2} \right] \\ K_0 &= \mu_0 S (NK_c U_m \delta_{\max})^2 \\ K_1 &= 4K_c^2 R^2 \delta_{\max}^2 \\ K_2 &= \mu_0^2 \omega^2 S^2 N^4 \\ b &= K_c \delta_{\max} - a \end{aligned} \quad (8)$$

Where a = the nominal working air gap, x = rotor displacement, δ_{max} = the maximum of working air gap.

From equation 8, the steady-state resultant force acting on the rotor is shown in Fig.4. It shows that the working air gap increasing results in the steady-state resultant force augmenting. If some reason causes the rotor leave its original position, the increasing magnetic force will draw it back. So the radial magnetic bearing proposed is stable in the steady-state condition,

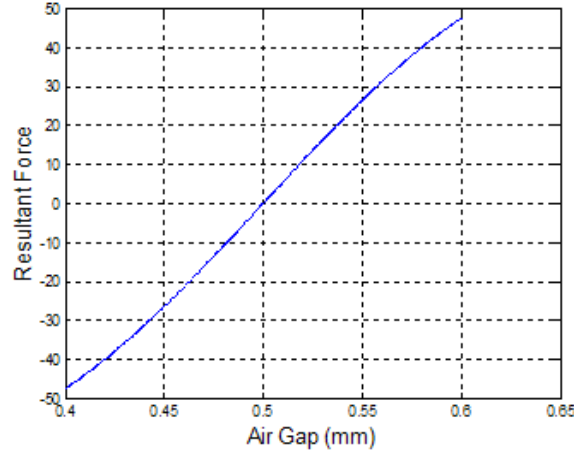


Fig.4 Relationship between working air gap and resultant force acting on rotor

In order to improve the dynamic state stability, the control winding, S_{CTR} , and a controller are adopted.

4 Stability analysis of the radial magnetic bearing

If the rotor displacement influence to stator current is taken into account, the balance of voltage in R, L, C loop can be written as

$$u(t) - L(t) \frac{d}{dt} i(t) - i(t) \frac{d}{dt} L(t) - \frac{1}{C} \int i(t) dt = i(t)R \quad (9)$$

The motion equation of the rotor is expressed as

$$F = m \frac{d^2}{dt^2} x(t) \quad (10)$$

According to the equation 8, 9 and 10, the dynamic model of the radial magnetic bearing proposed can be built with SIMULINK under no excitation in the control winding. See Fig.5.

For an example, $a=0.5\text{mm}$, $R=0.05 \Omega$, $f=1750\text{Hz}$, $N=42\text{T}$, $K_C=0.9$, $U_m=30\text{V}$, $m=2\text{kg}$ and $S=137\text{mm}^2$, the dynamic model of Fig.5 can be integrated into Fig.6 based on step response^[1]. The transfer function of Fig.6 system is as follows

$$G(s) = \frac{F(s)}{x(s)} = \frac{6.17 \times 10^{-7} S^2 + 1 \times 10^{-3} S + 1}{1.234 \times 10^{-6} S^4 + 2 \times 10^{-3} S^3 + 2 S^2 + 2.1 \times 10^6} \quad (11)$$

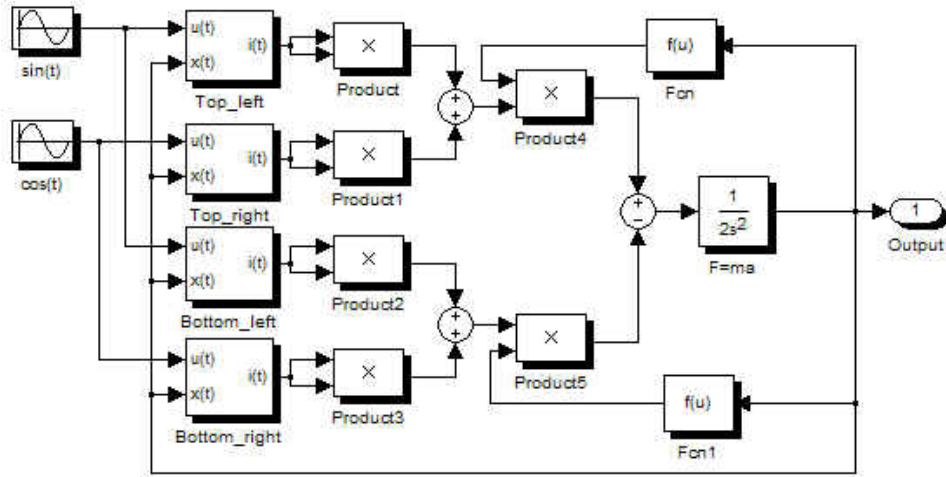


Fig.5 Dynamic model of the radial magnetic bearing proposed with SIMULINK

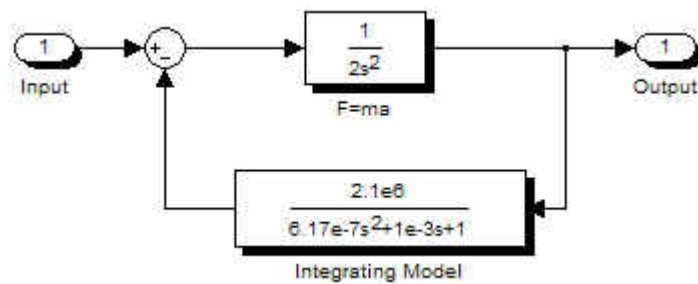


Fig.6 Simplified model of Fig.5 system

For the transfer function $G(s)$, Routh array^[2] can be calculated as follows

$$a_0 = 1.234 \times 10^{-6}$$

$$a_1 = 2 \times 10^{-3}$$

$$b_1 = 2$$

$$c_1 = -2.1 \times 10^3$$

Because c_1 is negative, the system dynamic state response is instability according to Routh criterion^[2].

5 Design of the control system

In order to enable the system stabilize, a controller is used in the system. The variation of working air gap is detected by measuring the difference between top right and bottom right stator winding current. Full wave rectifiers and 2nd-order Butterworth lowpass filters are adopted. See Fig.2.

The transfer function between working air gap and difference of currents for the example mentioned above can be integrated as follows

$$G_i(s) = \frac{D_c(s)}{x(s)} = \frac{1.7 \times 10^5}{1.95 \times 10^{-6} S^2 + 3.88 \times 10^{-3} S + 1} \quad (12)$$

The system structure inserted into a controller is shown in Fig.7.

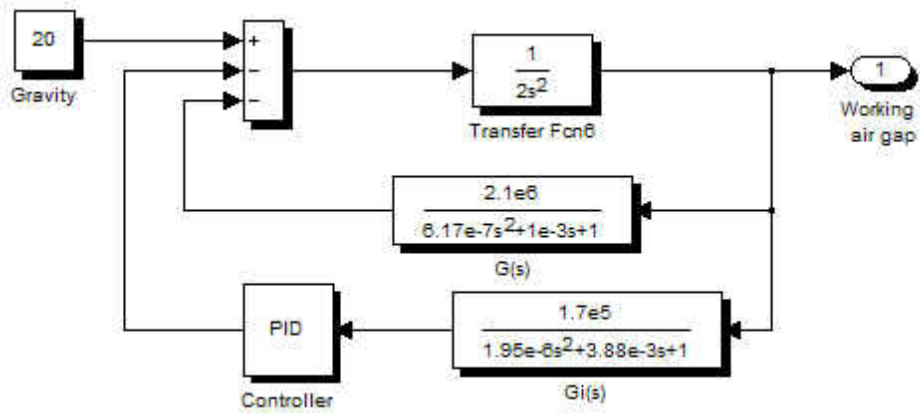
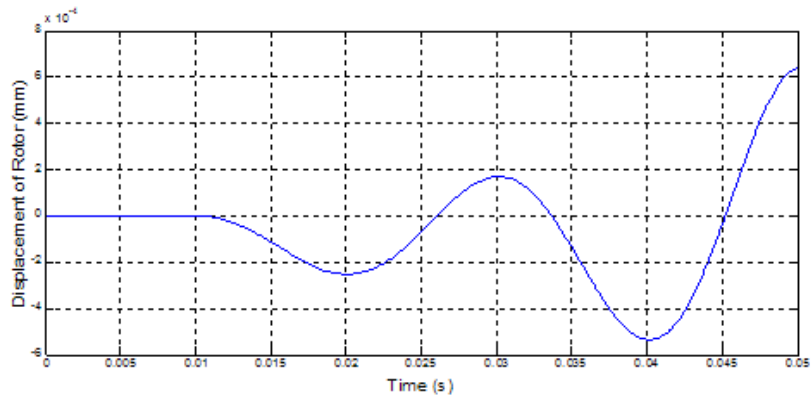


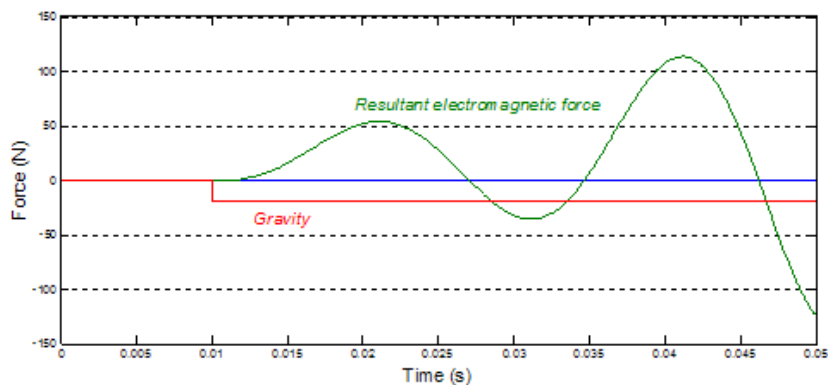
Fig.7 Control system of the radial magnetic bearing proposed

6 Simulation results

The simulation results are seen from Fig.8 to Fig.11.



(a) Displacement of the rotor



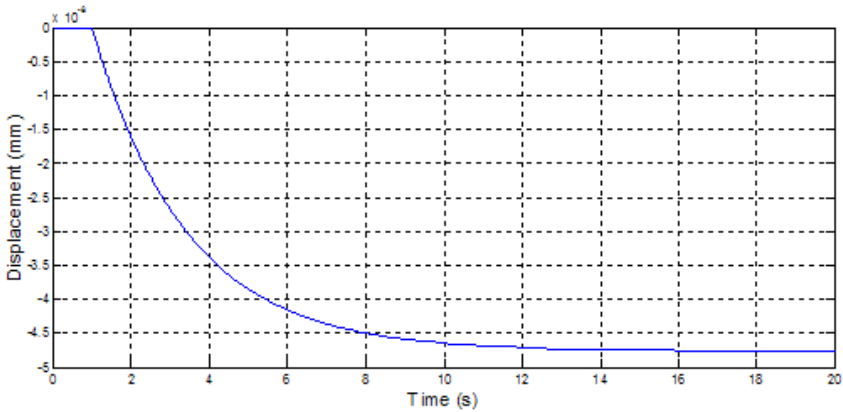
(b) Forces acting on rotor

Fig.8 Simulation results for Fig.6 system

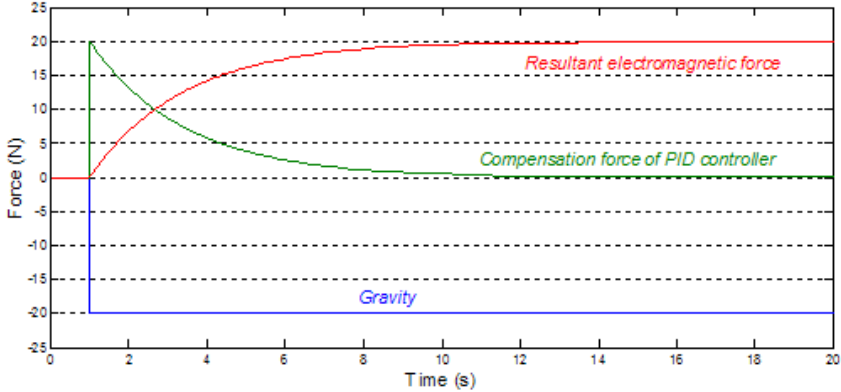
Fig.8 is the simulation results of the system shown in Fig.6. Fig.8a indicates the displacement

variation of the rotor with time in the case of gravity acting. Fig.8b gives the gravity and the changing of the resultant electromagnetic force. Because the resultant electromagnetic force or displacement of rotor is divergent, the system shown in Fig.6 is instable.

Fig.9 is the simulation results of the system with PD controller shown in Fig.7.



(a) Displacement of the rotor



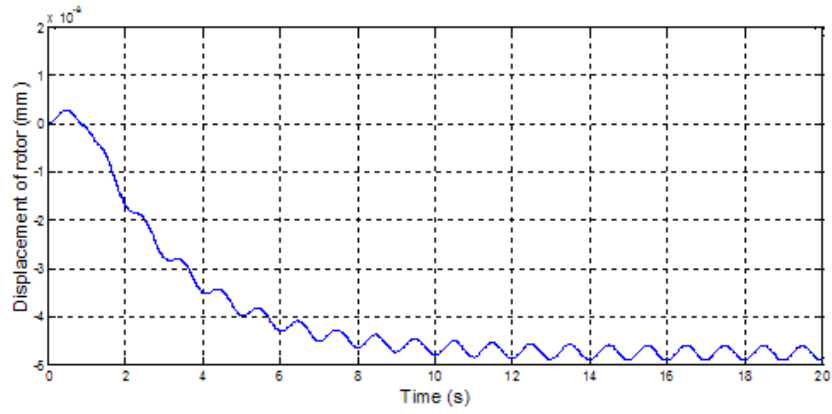
(b) Forces acting on rotor

Fig.9 Simulation results for Fig.7 system

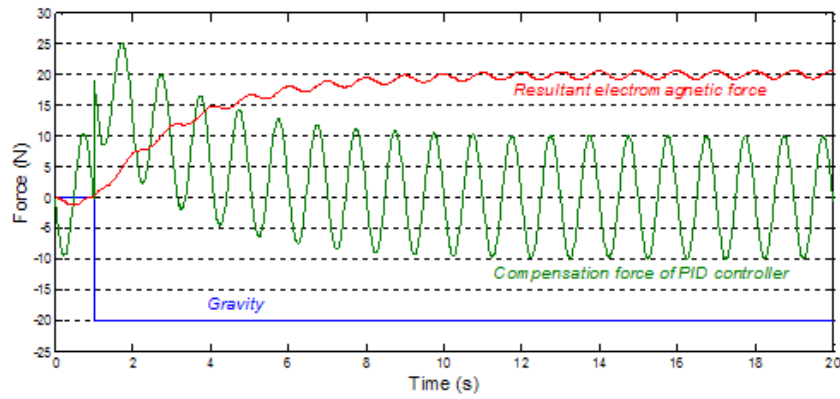
Fig.9a indicates the variation of the rotor displacement with time in the case of gravity acting. Fig.9b gives the gravity, the resultant electromagnetic force and the compensation force of PD controller. Because the PD control strategy is used in the system shown in Fig.7, the rotor displacement is leveled off. The system shown in Fig.7 becomes stable. The PD controller only used for compensating variation of disturbance force in the transient process. So it is a system with static error.

Fig.10 illustrates the simulation results in the case of the gravity and a sinusoidal disturbance force with a frequency of 1Hz and amplitude of 10N acting simultaneously.

Fig.11 gives the simulation results of the system shown in Fig.7 with PID controller. It shows that when a PID control strategy is adopted, the system is without static error.



a) Displacement of the rotor



(b) Forces acting on rotor

Fig.10 Simulation results for Fig.7 system with PD controller

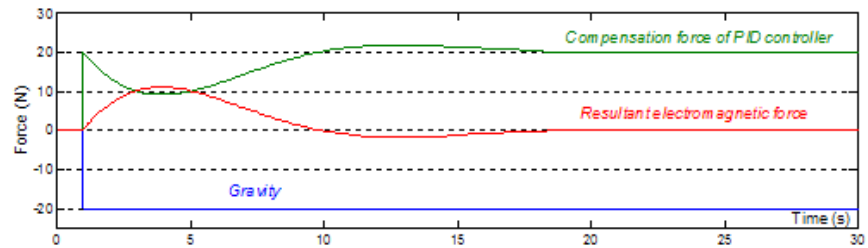
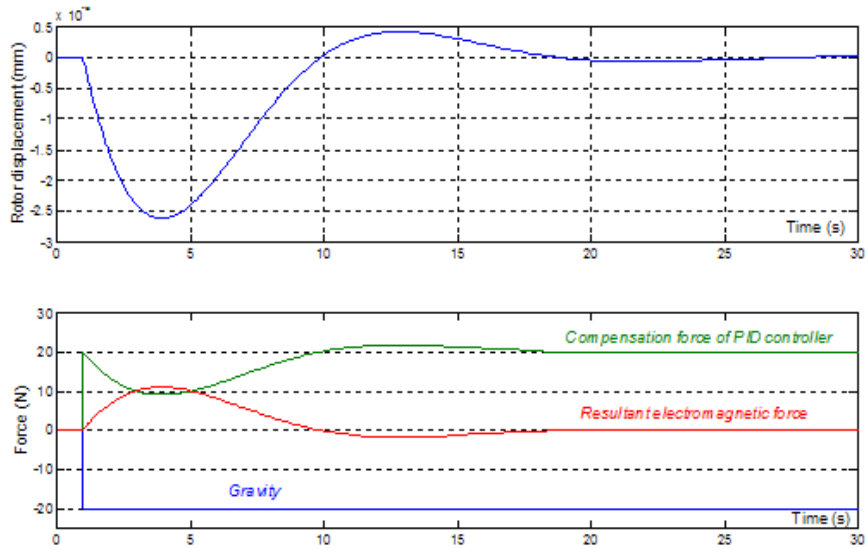


Fig.11 Simulation results for Fig.7 system with PID controller

7 Conclusion

Through studying on a novel radial magnetic bearing proposed in this paper, the following conclusions can be drawn.

- The proposed system without PD controller is instable though it is stable in the steady-state.
- Using PD control strategy, the system becomes stable in the dynamic state process, but it is a static error system.
- Because no displacement sensor needed, the structure of the radial magnetic bearing proposed is simplified and easy to control.
- The proposed radial magnetic bearing system is feasible

References

1. Manfred Morari. N. Lawrence Ricker. Model Predictive Control Tollbox User's Guide. MathWorks. Inc. 1998.
2. P. B. Deshpande. R. H. Ash. Computer Process Control with Advanced Control Applications, 2nd ed. ISA, 1988
3. Betschon, F. Knospe, C.R. Reducing magnetic bearing currents via gain scheduled adaptive control Mechatronics, IEEE/ASME Transactions on, Volume: 6 Issue: 4, Dec. 2001 Page(s): 437 -443.
4. Mukhopadhyay, S.C. Ohji, T. Iwahara, M. Yamada, S. Modeling and control of a new horizontal-shaft hybrid-type magnetic bearing. Industrial Electronics, IEEE Transactions on, Volume: 47 Issue: 1, Feb. 2000 Page(s): 100 -108.
5. Kasarda, M.E. Clements, J. Wicks, A.L.; Hall, C.D. Kirk, R.G. Effect of sinusoidal base motion on a magnetic bearing. Control Applications, 2000. Proceedings of the 2000 IEEE International Conference on, 25-27 Sept. 2000, Page(s): 144 -149
6. McMullen P T, S.Huynh C, Hayes R J. Combination radial-axial magnetic bearing [C]. In: Proc. 6th Int. Symp. Magnetic bearings, ETH Zurich, Switzerland, 2000: 473-478.